

Transfer of terrestrial carbon to and processing within drainage basins

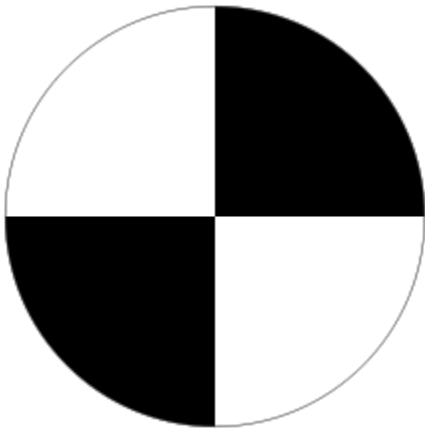
Pete Raymond

Yale School of Forestry and
Environmental Studies

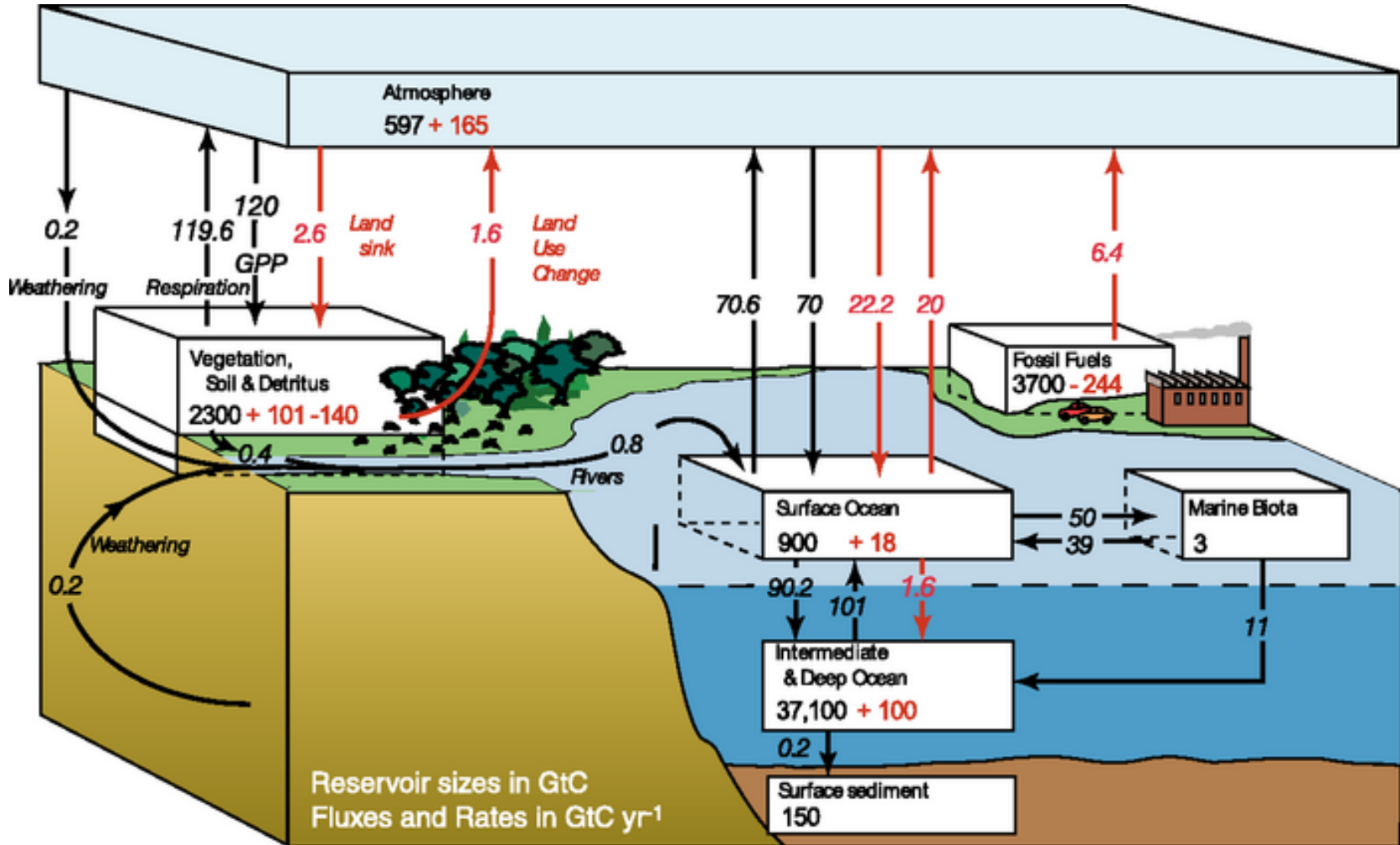
Angelo Secchi



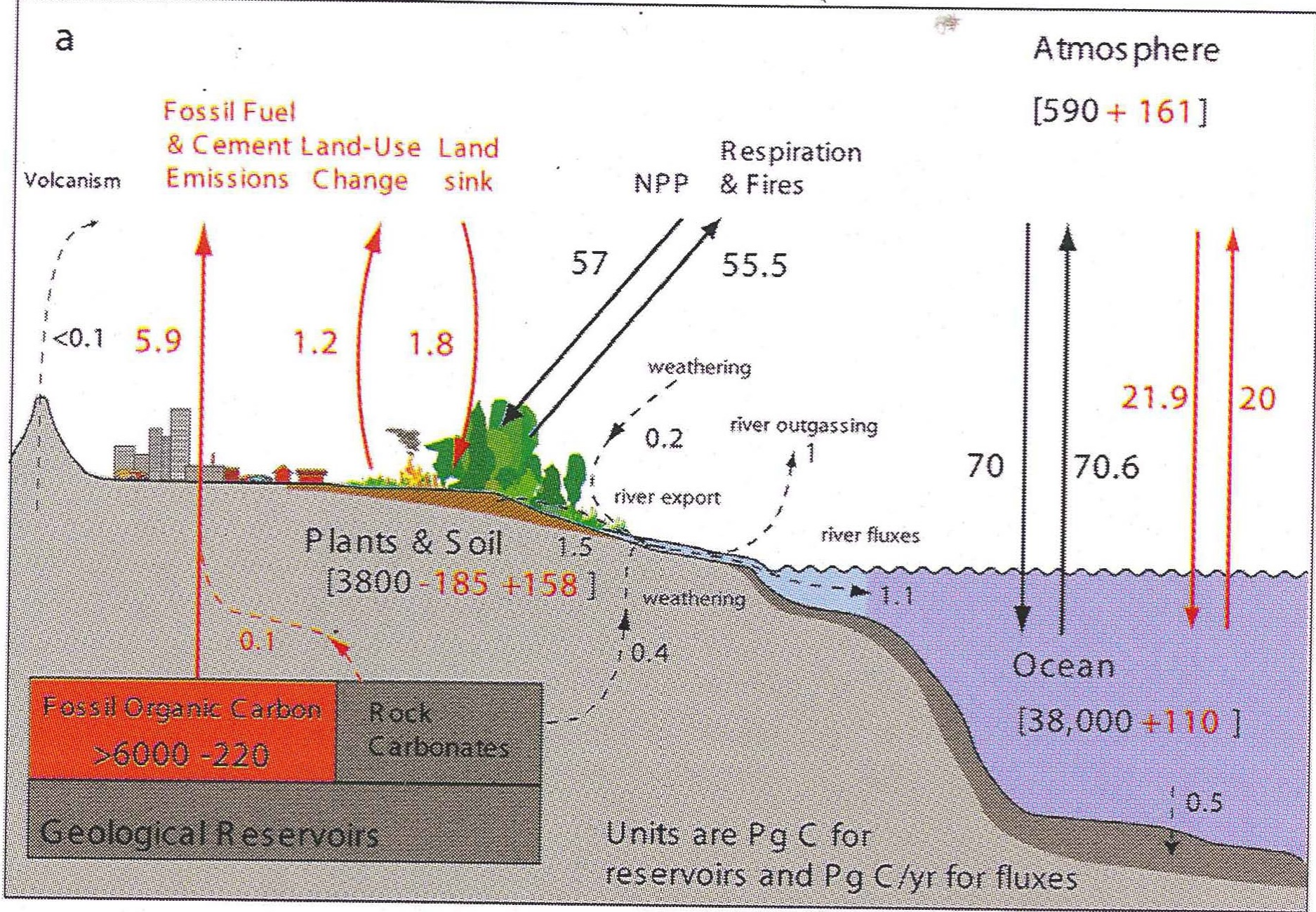
- First scientist to state authoritatively that the sun is a star
- Invented secchi disk for first measurement of ocean color.
- The first disk was lowered from the papal yacht, l'immacolata Concezion (Immaculate Conception), on April 20, 1865 (Carlson and Simpson, 1996).

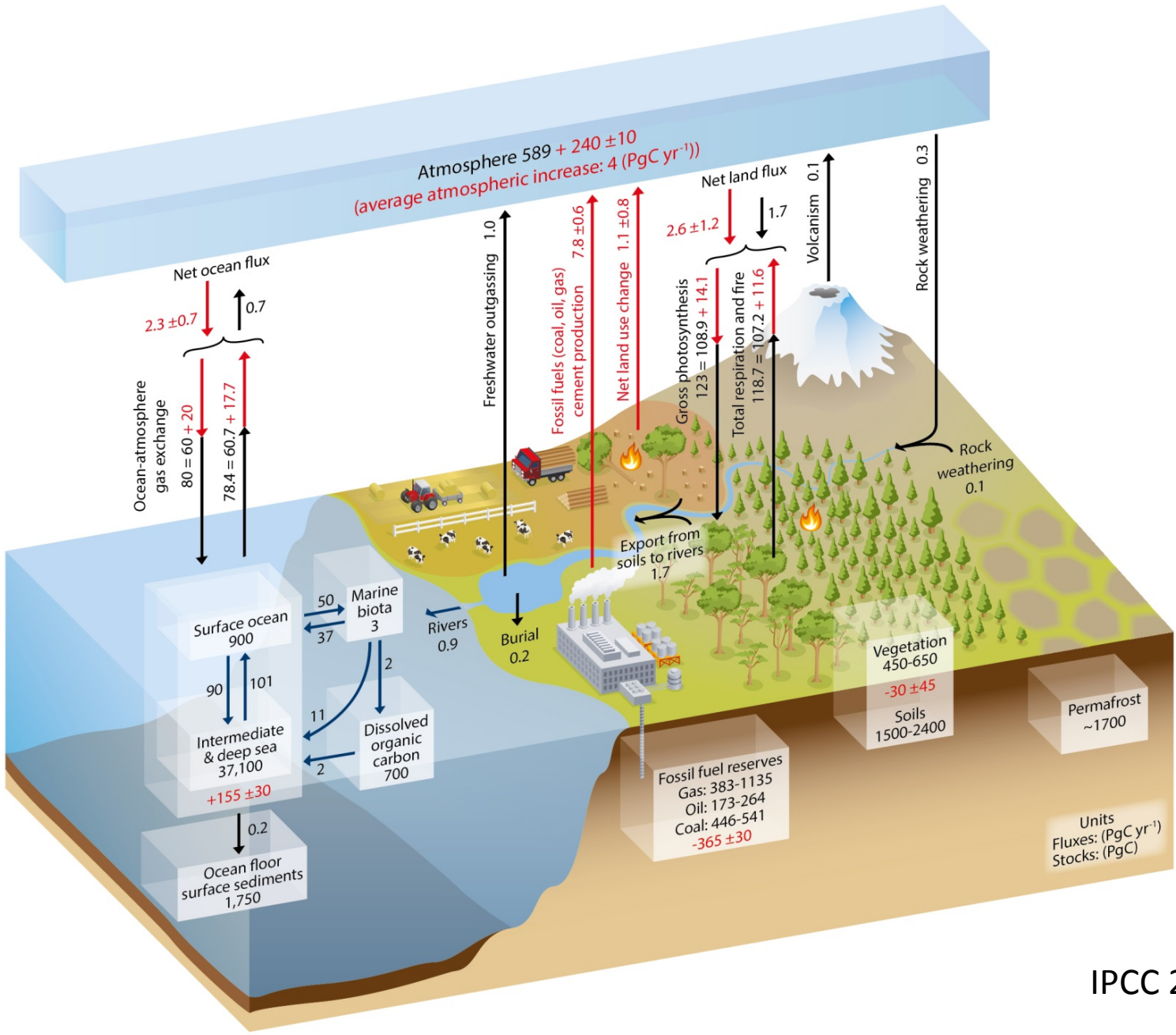


Evolution of Boundless C

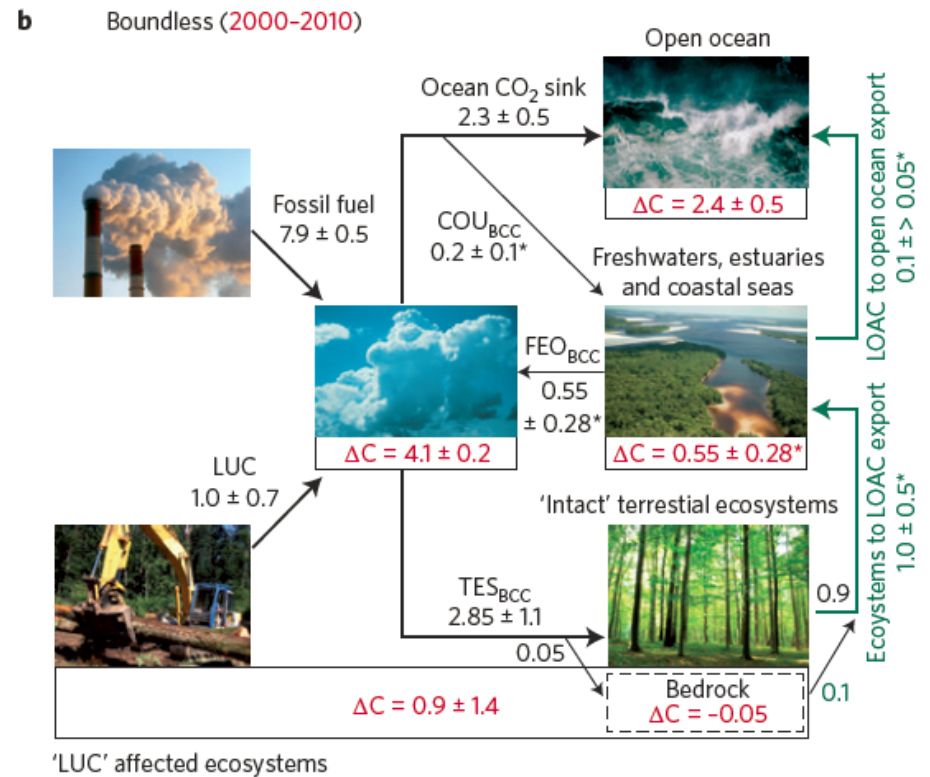
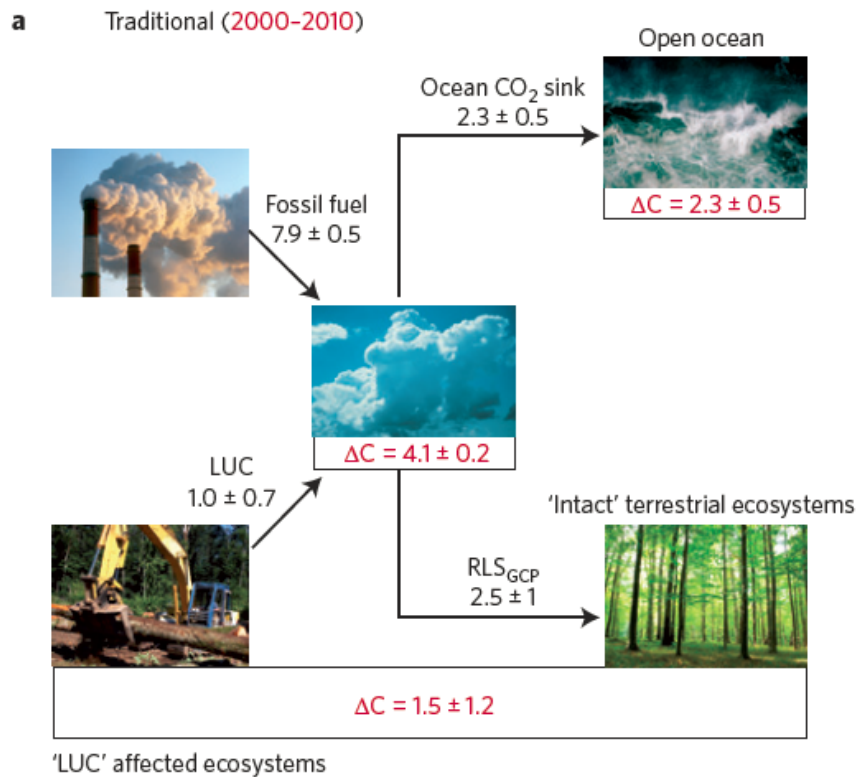


Sarmiento and Gruber (2002)



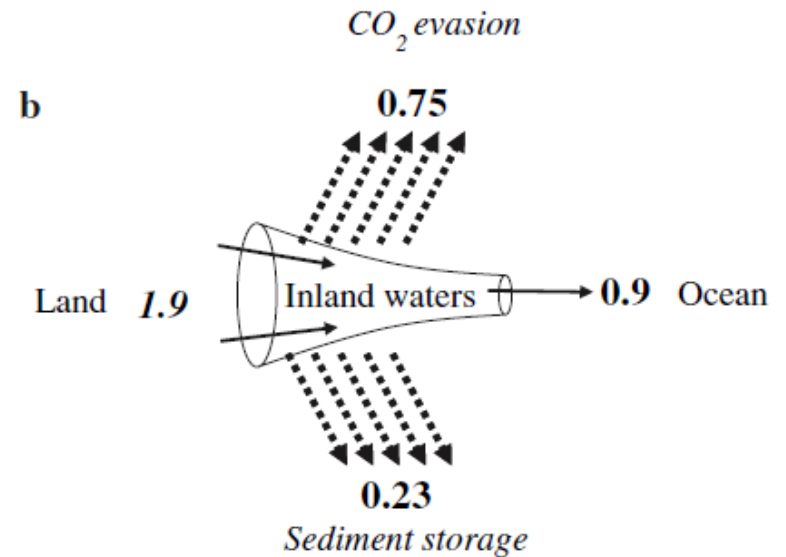
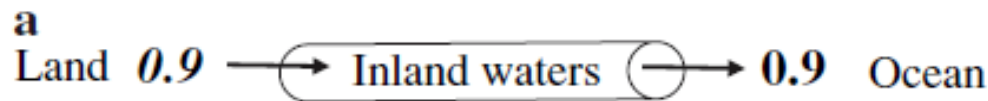


IPCC 2013



Regnier et al. 2013

The Active Pipe Model



Cole et al. 2007

Terrestrial Aquatic Linkages

Major Areas of Research

- Terrestrial Transport to Inland Waters
 - Hydrologic controls
 - Terrestrial Biological Controls
- Transport and Transformations during Transit
 - Major Processes
 - Removal/addition and change in composition/form
 - Impact on Inland Waters
- Impact on Receiving Coastal Waters

Riverine Transport to Ocean

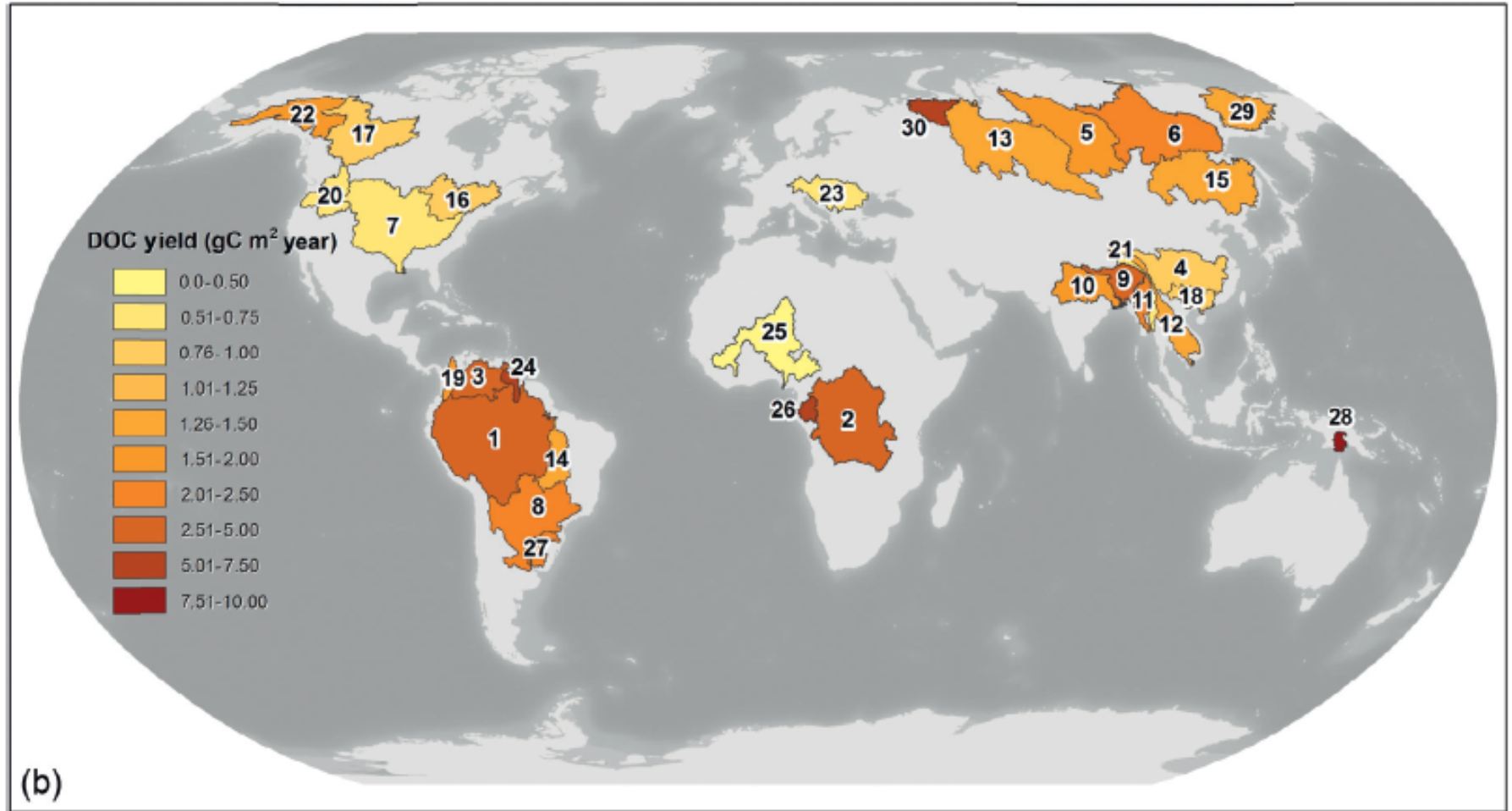


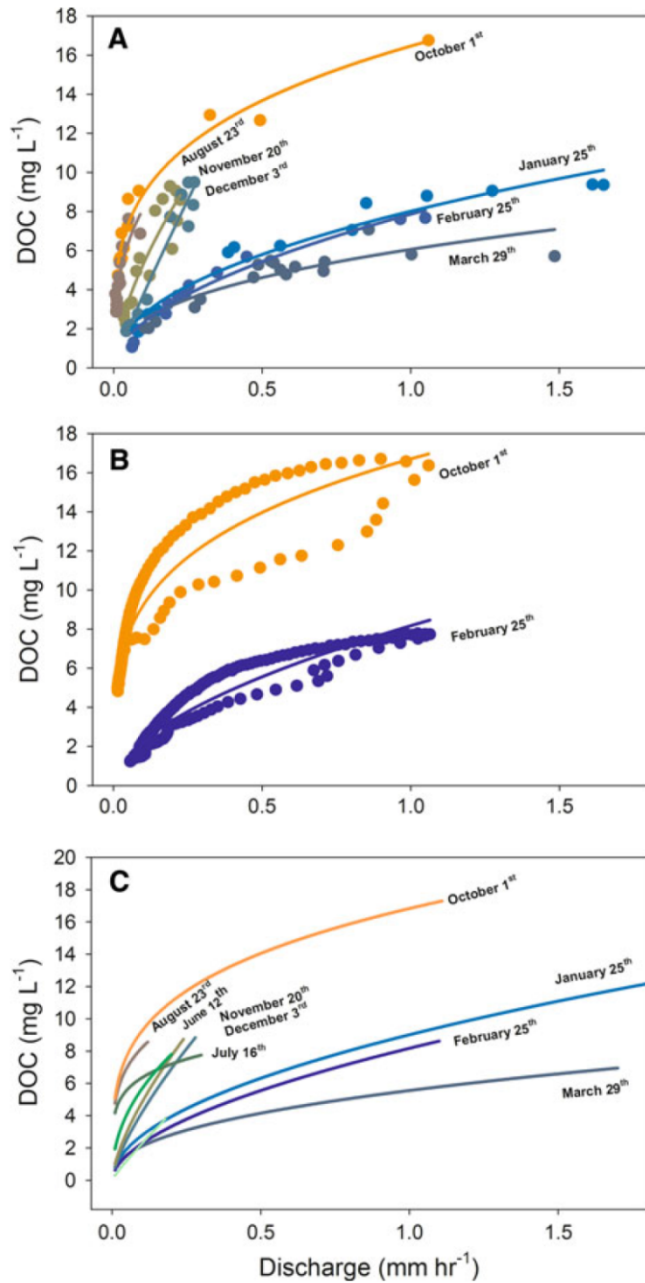
FIGURE 11.1 DOC fluxes (a) and yields (b) for the top 30 global rivers ranked by discharge. Data from Table 1.

Raymond and Spencer 2014

How much terrestrial C enters inland waters?

- Measurements
 - Need to focus on small watersheds
 - End-member land-use systems across climate gradients
 - Elucidate hot-spots (e.g., wetlands for DOC)
 - Need to sample hydrologic events, which are short in duration
- Models
 - Have to have strong hydrologic component
 - Need for both simple and complex models

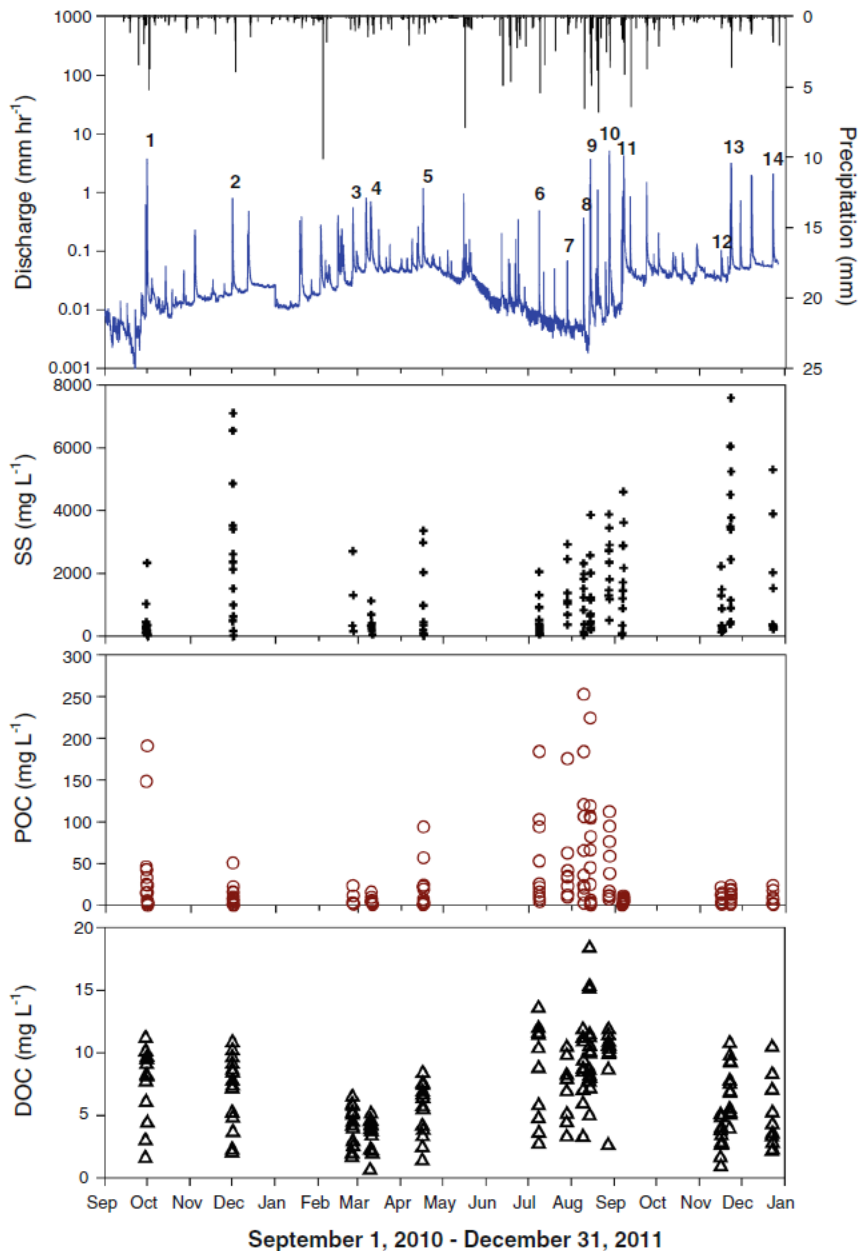
Terrestrial transfers: DOC Harvard Forest



- 60% of export occurs during 15 days of year

Wilson et al. 2014

DOC & POC Export with Storms: Atlantic Piedmont



Dhillon and Inamdar 2014

DOC Export with Storms: Brittany France

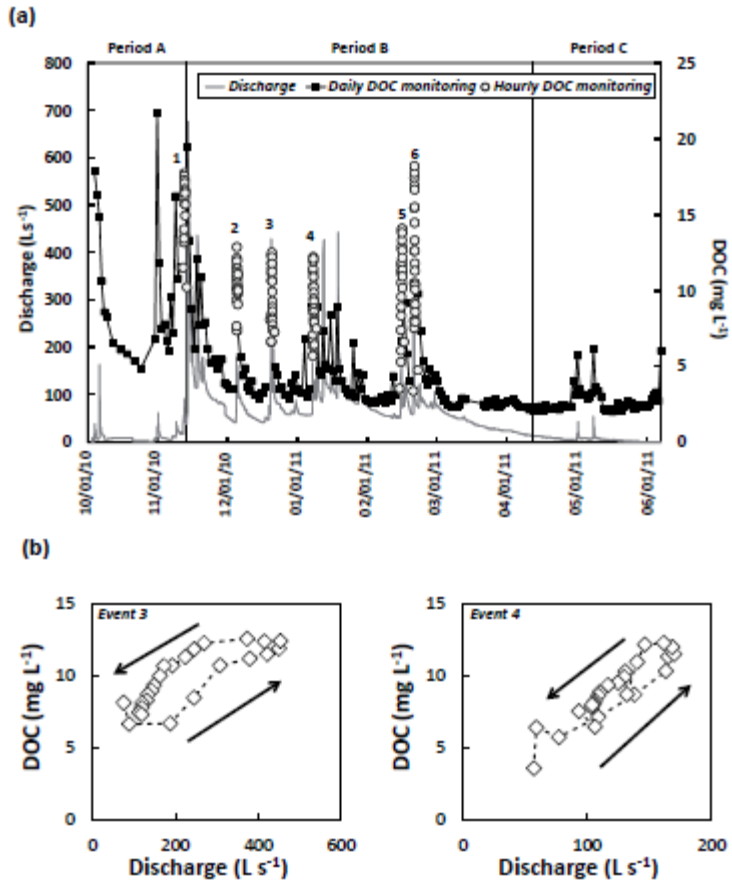
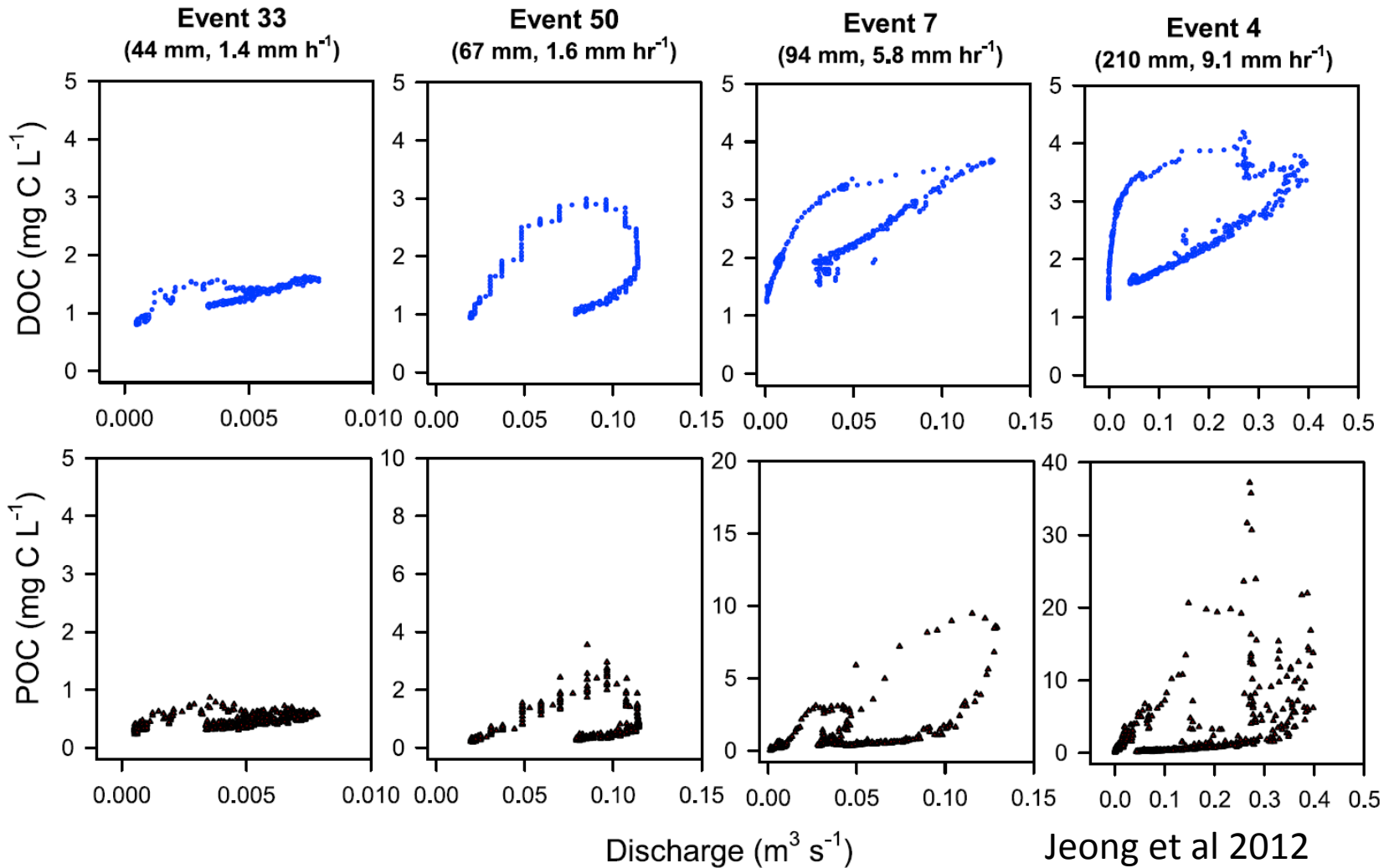


Figure 4. (a) Temporal variations in stream discharge and DOC concentrations at the catchment outlet during the study period and (b) example of DOC concentrations versus discharge showing hysteresis patterns (arrows indicate chronology). Monitored storm events are indicated by numbers in box (a).

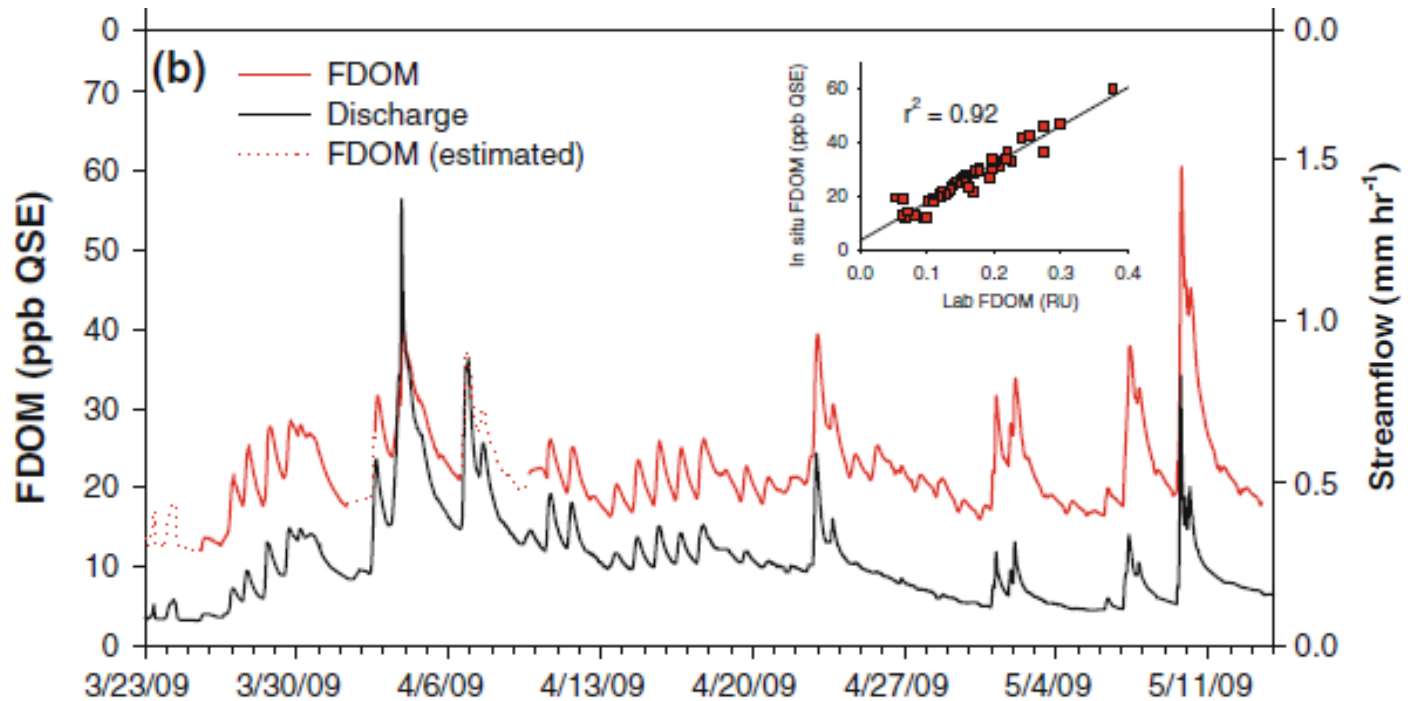


Lambert et al. 2014

DOC & POC Export with Storms: South Korea

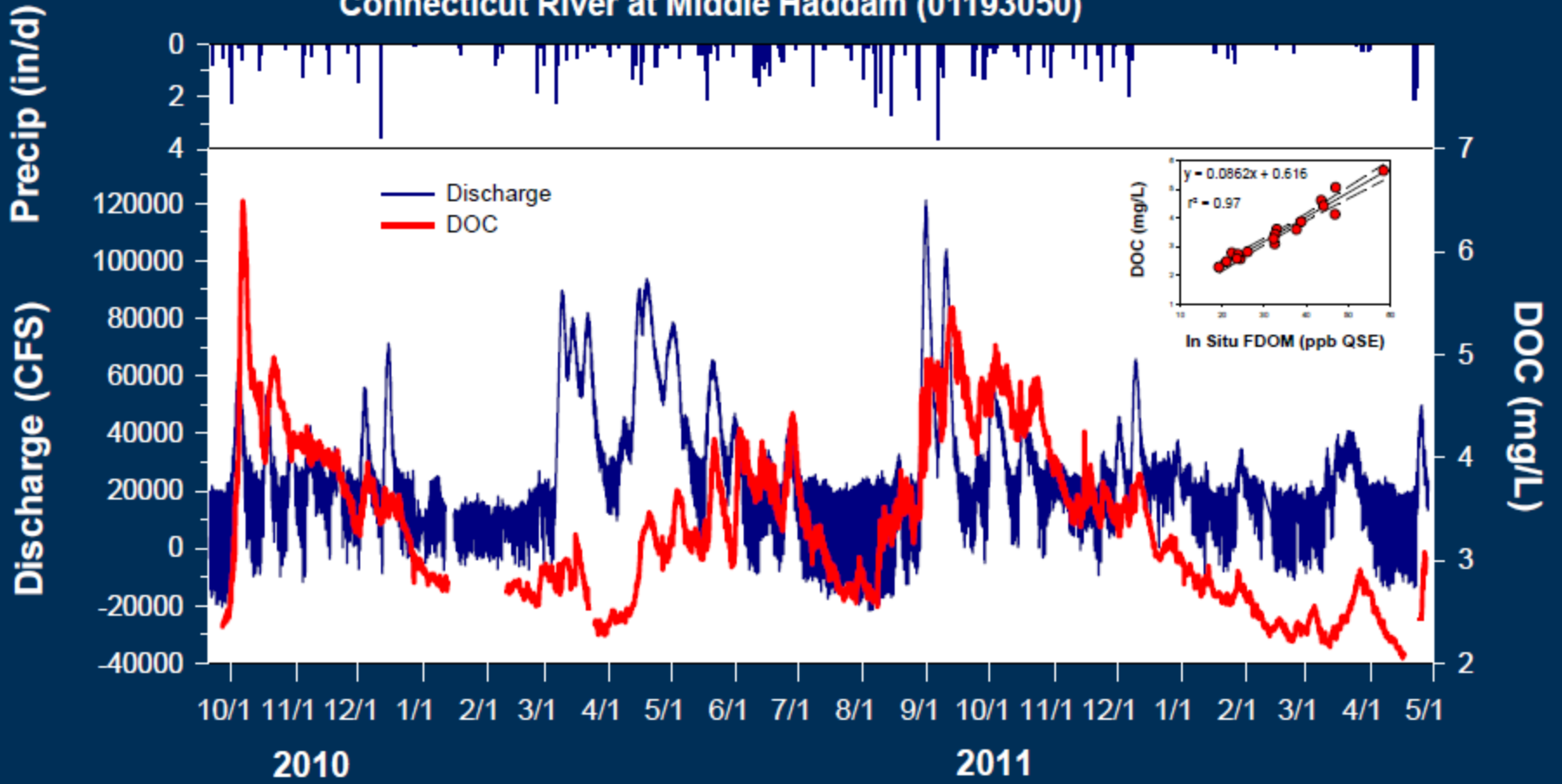


DOC Export with Storms: Sleepers River VT



Pellerin et al. 2012

Connecticut River at Middle Haddam (01193050)



Pellerin et al

LAND USE AND CLIMATE VARIABILITY AMPLIFY CARBON, NUTRIENT, AND CONTAMINANT PULSES: A REVIEW WITH MANAGEMENT IMPLICATIONS¹

Sujay S. Kaushal, Paul M. Mayer, Philippe G. Vidon, Rose M. Smith, Michael J. Pennino, Tamara A. Newcomer, Shuiwang Duan, Claire Welty, and Kenneth T. Belt²

ABSTRACT: Nonpoint source pollution from agriculture and urbanization is increasing globally at the same time climate extremes have increased in frequency and intensity. We review >200 studies of hydrologic and gaseous fluxes and show how the interaction between land use and climate variability alters magnitude and frequency of carbon, nutrient, and greenhouse gas pulses in watersheds. Agricultural and urban watersheds respond similarly to climate variability due to headwater alteration and loss of ecosystem services to buffer runoff and temperature changes. Organic carbon concentrations/exports increase and organic carbon quality changes with runoff. Nitrogen and phosphorus exports increase during floods (sometimes by an order of magnitude) and decrease during droughts. Relationships between annual runoff and nitrogen and phosphorus exports differ across land use. CH₄ and N₂O pulses in riparian zones/floodplains predominantly increase with: flooding, warming, low oxygen, nutrient enrichment, and organic carbon. CH₄, N₂O, and CO₂ pulses in streams/rivers increase due to similar factors but effects of floods are less known compared to base flow/droughts. Emerging questions include: (1) What factors influence lag times of contaminant pulses in response to extreme events? (2) What drives resistance/resilience to hydrologic and gaseous pulses? We conclude with eight recommendations for managing watershed pulses in response to interactive effects of land use and climate change.

(KEY TERMS: eutrophication; water quality; hypoxia; nonpoint source pollution; methane; nitrous oxide; carbon dioxide; restoration; wetlands; best management practices.)

Kaushal, Sujay S., Paul M. Mayer, Philippe G. Vidon, Rose M. Smith, Michael J. Pennino, Tamara A. Newcomer, Shuiwang Duan, Claire Welty, and Kenneth T. Belt, 2014. Land Use and Climate Variability Amplify Carbon, Nutrient, and Contaminant Pulses: A Review with Management Implications. *Journal of the American Water Resources Association* (JAWRA) 50(3): 585-614. DOI: 10.1111/jawr.12204

Modeling DOM Responses to Climate Change in New England

- Hydrologic Responses
 - Understanding storm flow through surficial soils is key to modeling loadings (Sebestyen et al. (2009))
 - Storm flow through surficial soils will increase in winter due to increased dormant season precipitation due to climate change.
 - Increase in the number of large events will increase DOM transport (Raymond et al. in review)
- Biologic Processes
 - Stream water losses decrease due to declines in litterfall and soil C mineralization rates with future climate change (Campbell et al. 2009)

Enhanced transfer of terrestrially derived carbon to the atmosphere in a flooding event

Thomas S. Bianchi,¹ Fenix Garcia-Tigreros,¹ Shari A. Yvon-Lewis,¹ Michael Shields,¹ Heath J. Mills,¹ David Butman,² Christopher Osburn,³ Peter Raymond,² G. Christopher Shank,⁴ Steven F. DiMarco,¹ Nan Walker,⁵ Brandi Kiel Reese,^{1,9} Ruth Mullins-Perry,¹ Antonietta Quigg,^{1,6} George R. Aiken,⁷ and Ethan L. Grossman⁸

Received 26 November 2012; revised 14 October 2012; accepted 21 November 2012; published 8 January 2013.

between soil/plant litter and aquatic carbon pools. Here we demonstrate that the summer 2011 flood in the Mississippi River basin, caused by extreme precipitation events, resulted in a “flushing” of terrestrially derived dissolved organic carbon (TDOC) to the northern Gulf of Mexico. Data from the lower Atchafalaya and Mississippi rivers showed that the DOC flux to the northern Gulf of Mexico during this flood was significantly higher than in previous years. We also show that consumption of radiocarbon-modern TDOC by bacteria in floodwaters in the lower Atchafalaya River and along the adjacent shelf contributed to northern Gulf shelf waters changing from a net sink to a net source of CO₂ to the atmosphere in June and August 2011. This work shows that

Storm Impacts on Receiving Waters

RESEARCH ARTICLE

10.1002/2013JC009424

Key Points:

- Surface tDOC concentrations are retrieved using ocean-color remote sensing
- tDOC cross-shelf export is sporadic and exhibits large interannual variability
- tDOC cross-shelf export is enhanced during years of anomalously high discharge

Correspondence to:

C. G. Fichot,
cgfichot@gmail.com

Citation:

Fichot, C. G., S. E. Lohrenz, and R. Benner (2014), Pulsed, cross-shelf export of terrigenous dissolved organic carbon to the Gulf of Mexico, *J. Geophys. Res. Oceans*, 119, 1176–1194, doi:10.1002/2013JC009424.

Received 10 SEP 2013

Accepted 18 JAN 2014

Accepted article online 28 JAN 2014

Published online 20 FEB 2014

Pulsed, cross-shelf export of terrigenous dissolved organic carbon to the Gulf of Mexico

Cédric G. Fichot^{1,2}, Steven E. Lohrenz³, and Ronald Benner^{1,2}

¹Marine Science Program, University of South Carolina, Columbia, South Carolina, USA, ²Department of Biological Sciences, University of South Carolina, Columbia, South Carolina, USA, ³Department of Estuarine and Ocean Sciences, School for Marine Science and Technology, University of Massachusetts, Dartmouth, Massachusetts, USA

Abstract The export of terrigenous dissolved organic carbon (tDOC) and other river-borne material across the continental shelf boundary has important ramifications for biological productivity and the cycling of continentally derived bioelements in the ocean. Recent studies revealed the 275–295 nm spectral slope coefficient of chromophoric dissolved organic matter (CDOM), $S_{275-295}$, is a reliable tracer for terrigenous dissolved organic carbon (tDOC) in river-influenced ocean margins. Here an empirical algorithm for the accurate retrieval of $S_{275-295}$ from ocean color was developed and validated using in situ optical properties collected seasonally in the northern Gulf of Mexico. This study also demonstrated $S_{275-295}$ is a robust proxy for tDOC concentration in this environment, thereby providing a means to derive surface tDOC concentrations on synoptic scales and in quasi-real time using remote sensing. The resulting tDOC-algorithm was implemented using *Aqua*-MODIS in a retrospective analysis of surface tDOC concentrations over the northern Gulf of Mexico between July 2002 and June 2013. Large pulses of tDOC were observed in continental-slope surface waters off the Mississippi River delta, indicating cross-shelf export of tDOC was sporadic and exhibited considerable interannual variability. Favorable winds following an anomalously high discharge from the Mississippi-Atchafalaya river system always coincided with a major export event, and in general, cross-shelf export was enhanced during years of anomalously high discharge. The tDOC-algorithm will find applicability in the assessment of future climate- and human-induced changes in tDOC export, in biogeochemical models of the continental shelf, and in the validation of high-resolution coastal models of buoyancy-driven shelf circulation.



Contents lists available at ScienceDirect

Estuarine, Coastal and Shelf Science

journal homepage: www.elsevier.com/locate/ecss



Modeling the transport of freshwater and dissolved organic carbon in the Neuse River Estuary, NC, USA following Hurricane Irene (2011)

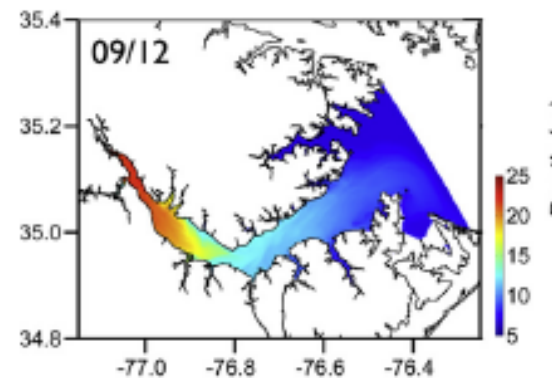
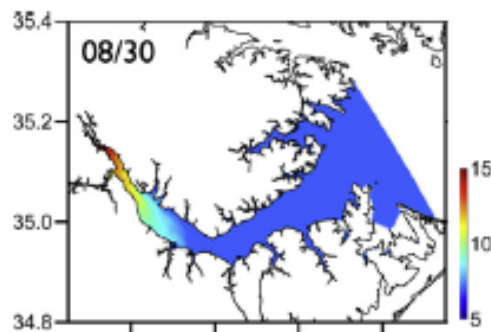


Matthew M. Brown^a, Ryan P. Mulligan^b, Richard L. Miller^{a,c,*}

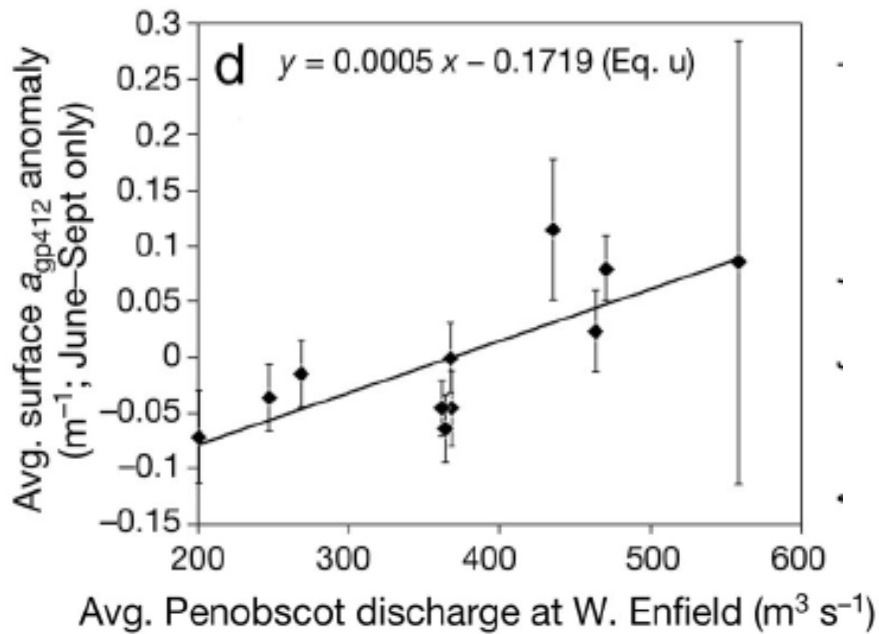
^aDepartment of Geological Sciences, East Carolina University, Greenville, NC 27858, USA

^bDepartment of Civil Engineering, Queen's University, Kingston, Ontario, Canada K7L 3N6

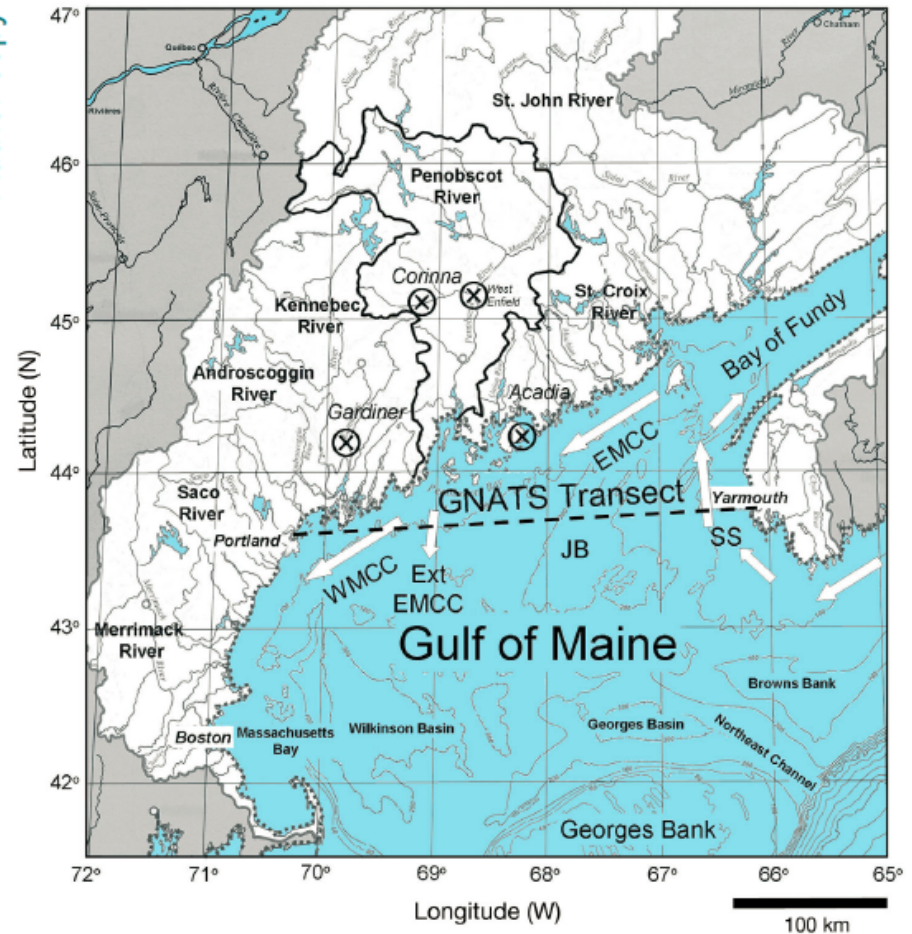
^cInstitute for Coastal Science and Policy, East Carolina University, Greenville, NC 27858, USA



Gulf of Maine Impacts

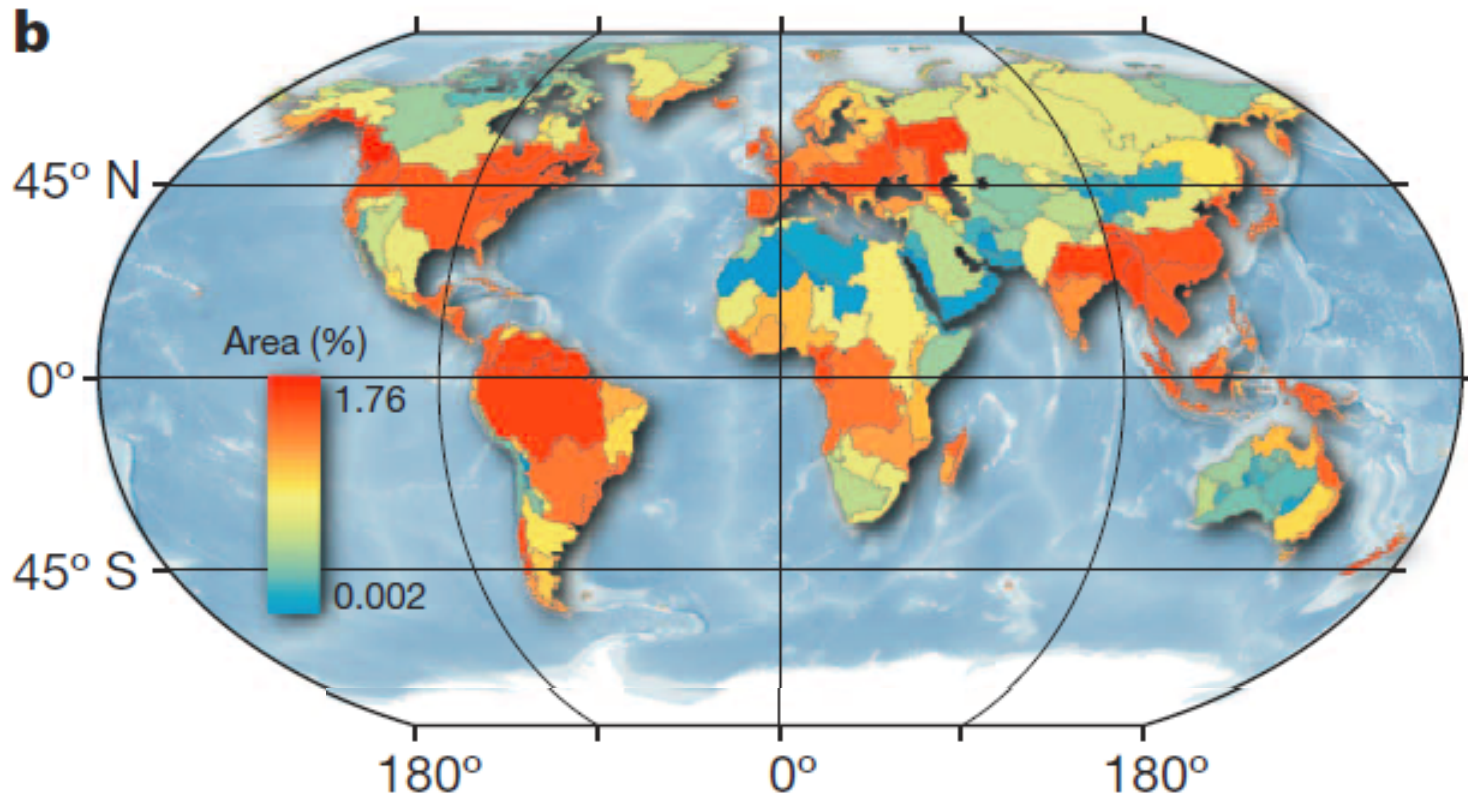


Author copy



Balch et al 2012

Transformations

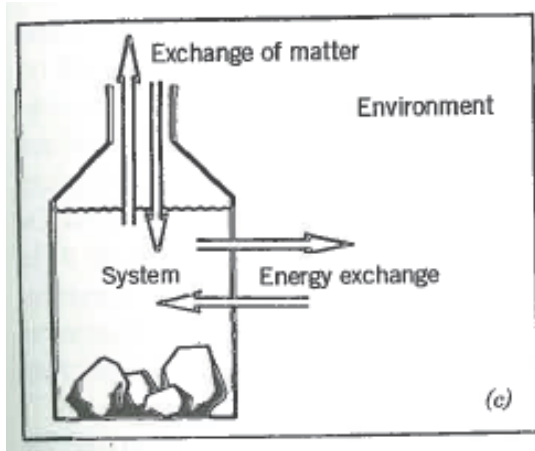


Inland Water CO₂ Efflux- 2.2Gt yr⁻¹

Raymond et al 2013

Regional/Global CO₂ Evasion

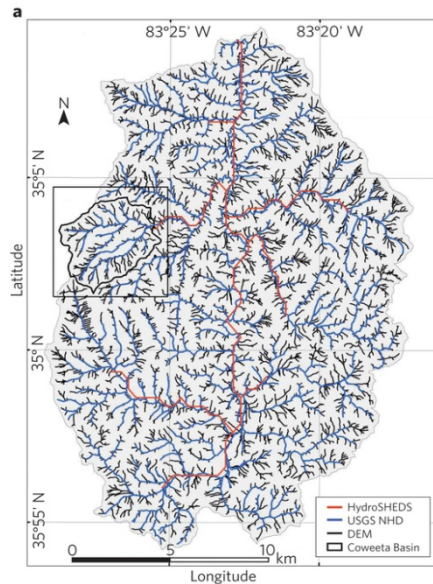
CO₂ Concentration
Gradient



Stumm and Morgan

X

Surface
Area



X

X

Gas Transfer
Velocity



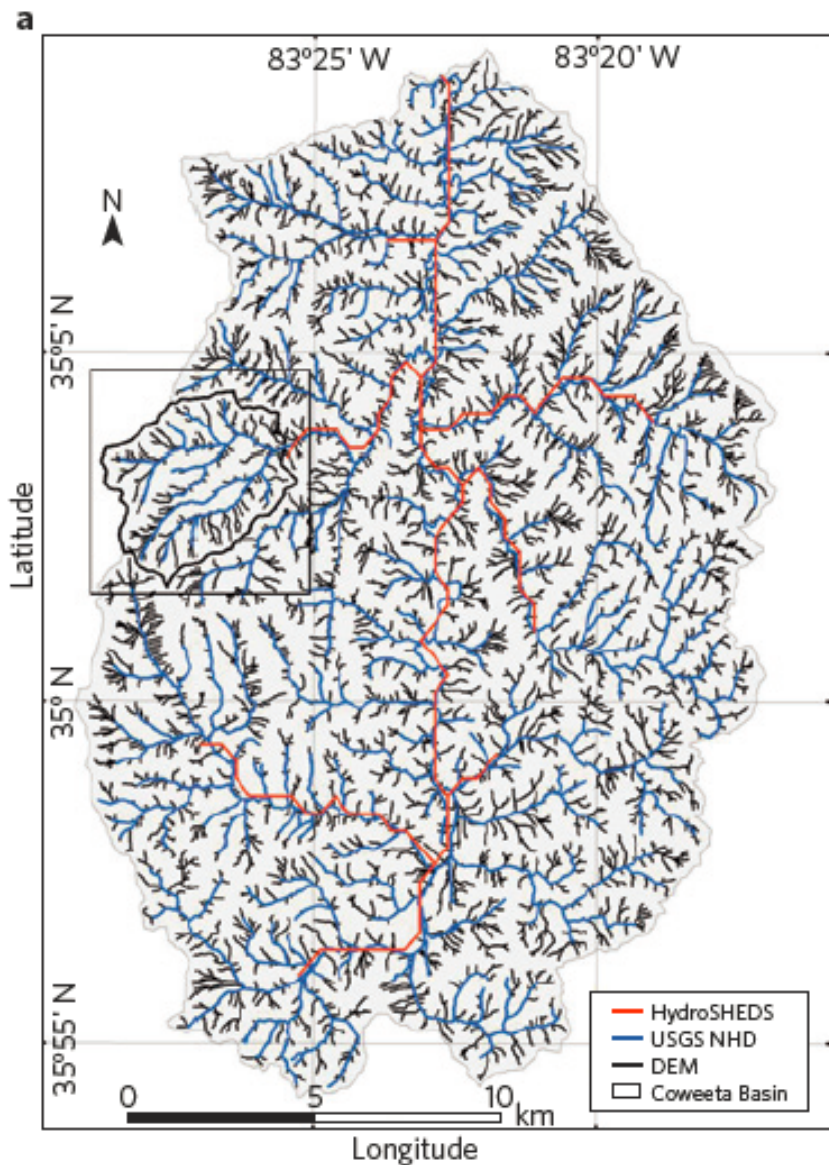
X

Benstead and Leigh, 2012

Surface Area

- Very few estimates of global stream/river surface area
- Estimate from length and width
- Spatial length products (e.g. HydroSHEDS and NHDplus) advancing quickly
- Width estimates and measurements also advancing quickly

Stream Surface Area - Length



- Difficult to determine when streams begin, lake-stream connections, ephemeral streams, wetland/floodplain connectivity

Benstead and Leigh 2012

Hydraulic “Primer”

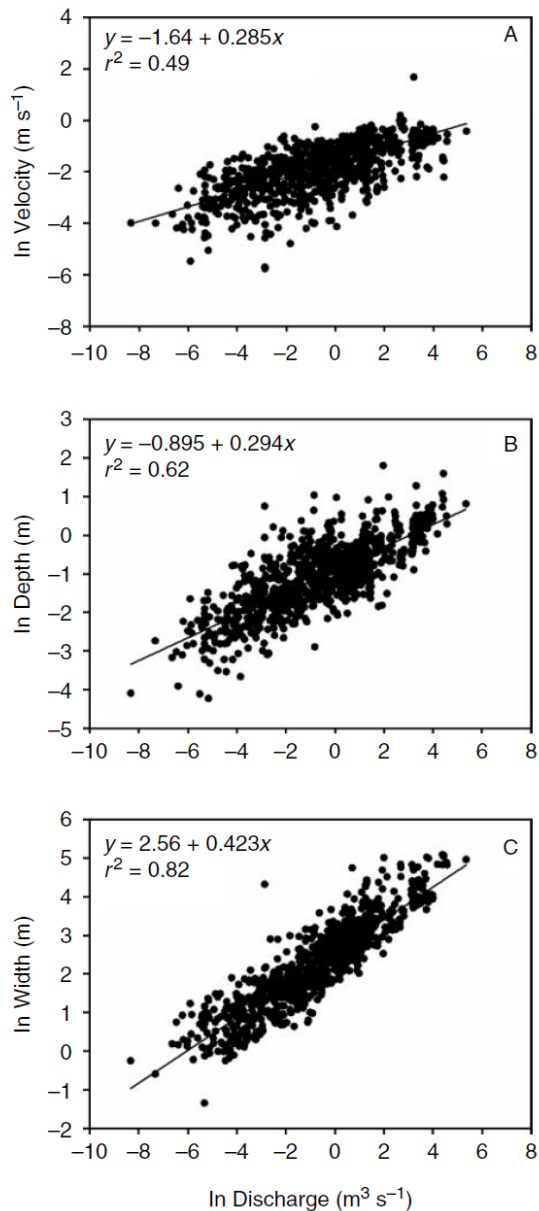


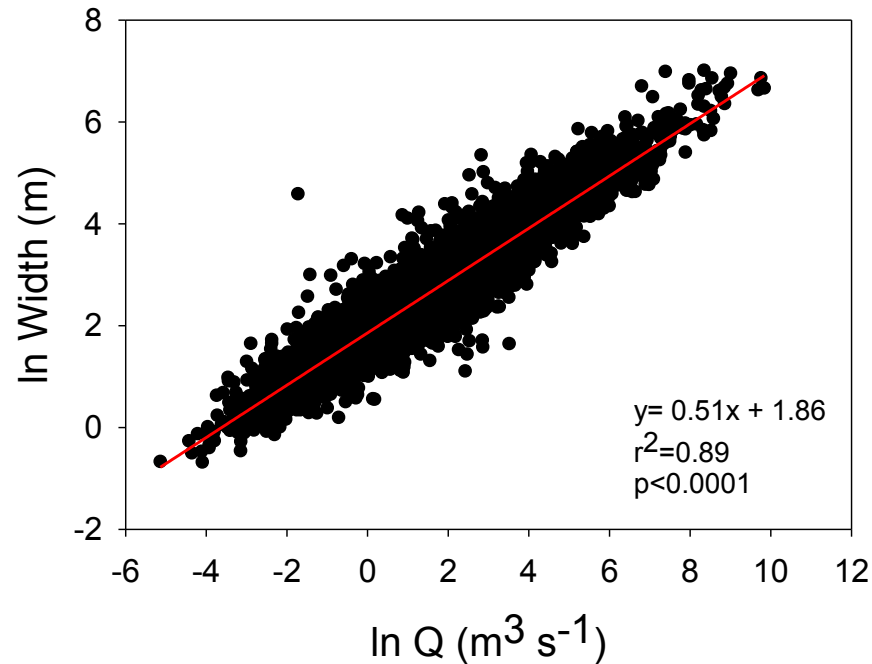
Fig. 1 Hydraulic geometry relationships for streams and rivers of this study. Presented are the relationships between discharge and velocity (A), depth (B), and width (C).

Raymond et al. 2012

- Discharge (Q) = Width * Velocity * Depth
- $W = aQ^b$
- $V = cQ^d$
- $D = eQ^f$
- $b+d+f=1$
- $a*c*e=1$

Stream Surface Area- Width

Comparing Two Data Sets



Raymond et al. 2013 from USGS data

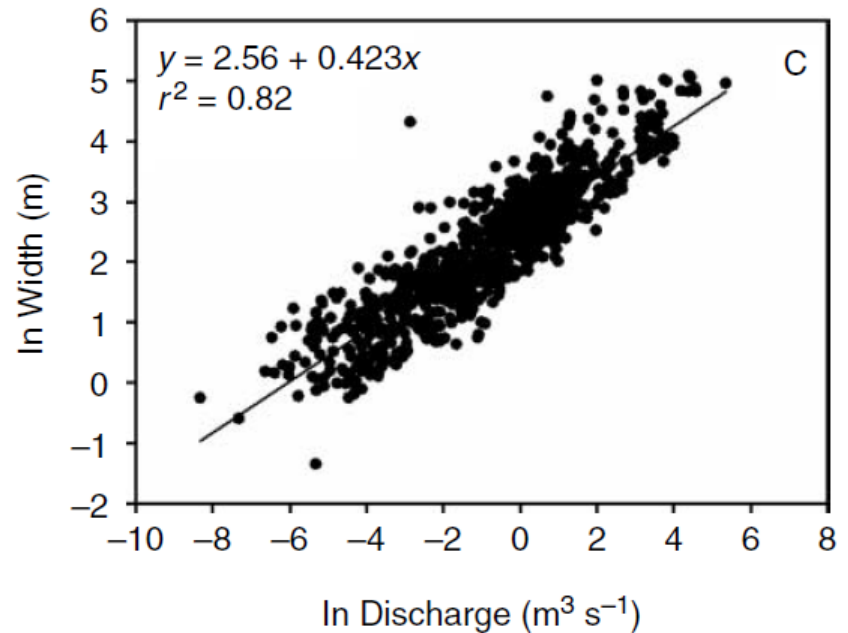
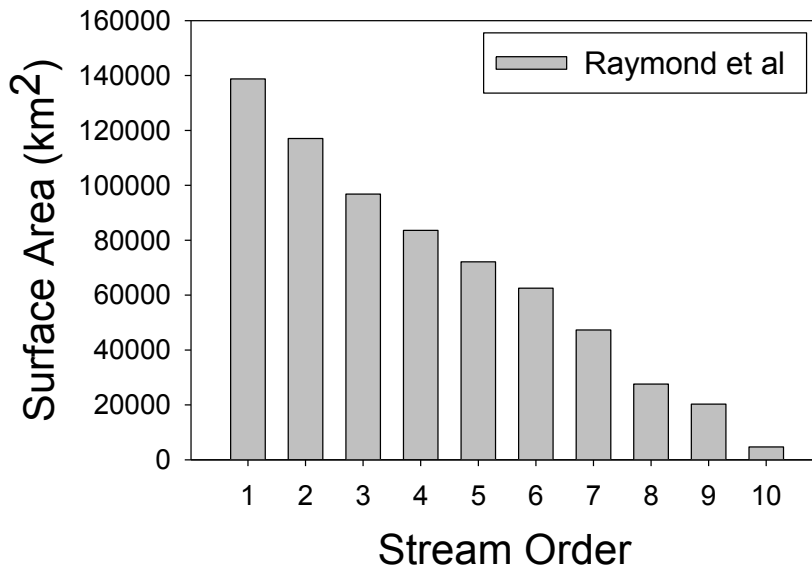
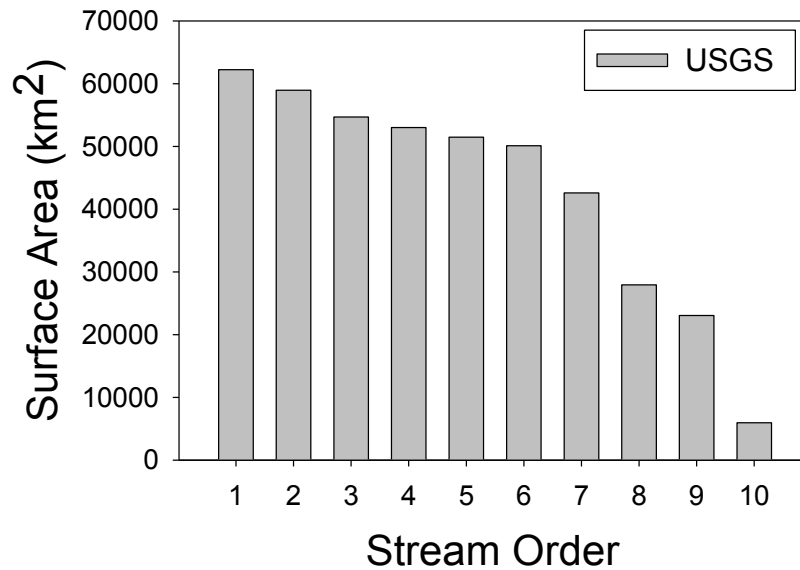


Fig. 1 Hydraulic geometry relationships for streams and rivers of this study. Presented are the relationships between discharge and velocity (A), depth (B), and width (C).

Raymond et al. 2012

$$W = aQ^b$$



Global surface area by stream order

- Larger role of small streams with Raymond et al.
- Global Surface area = 670,000km² versus 430,000km²

Stream Gas Transfer Velocity (k_{600})

47 • Gas transfer velocity and hydraulic geometry • Raymond et al.

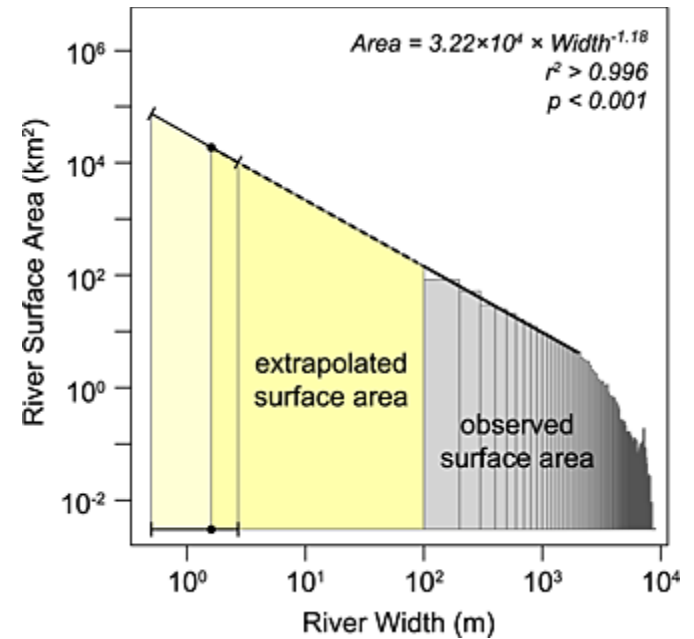
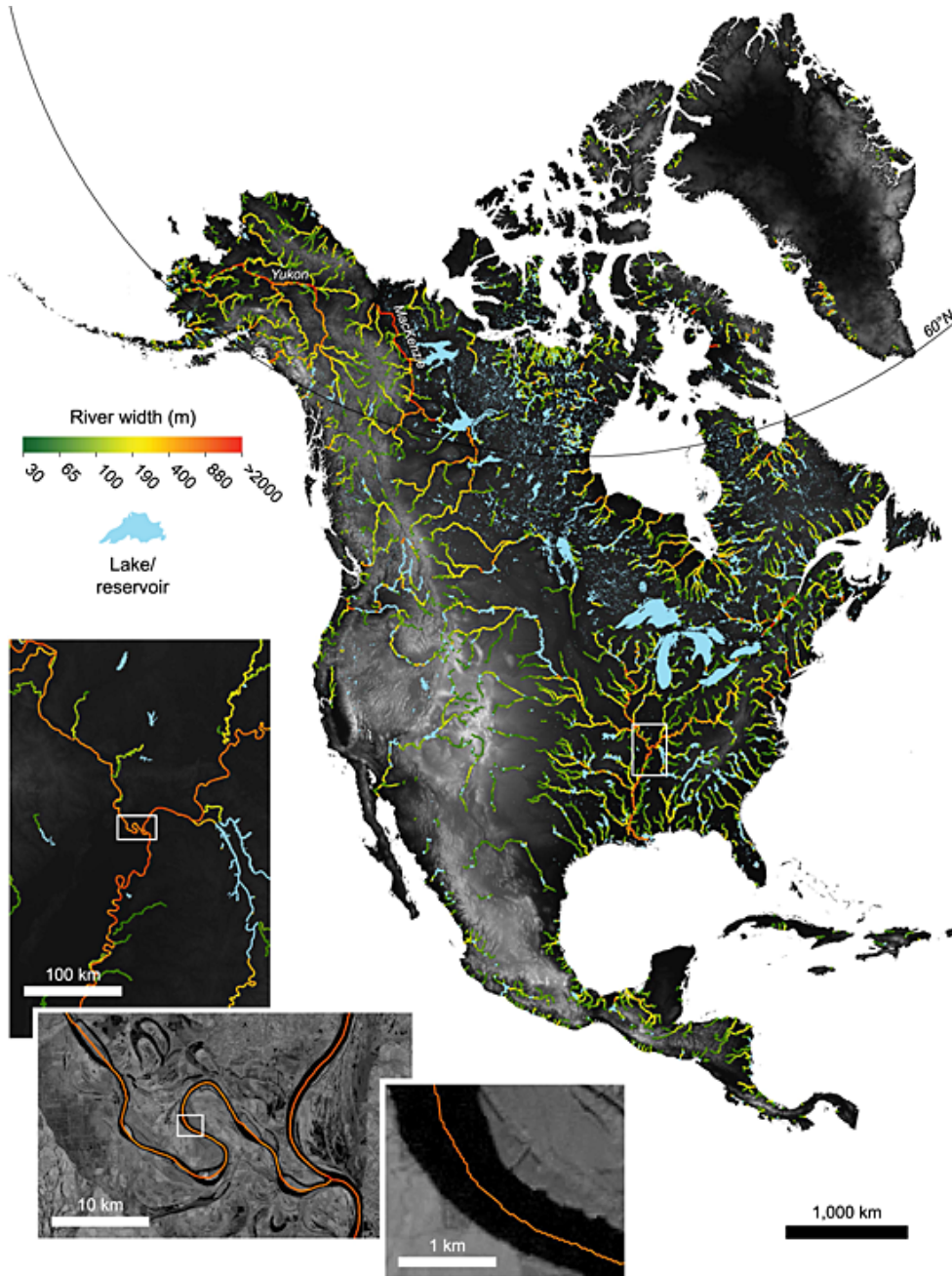
Table 2 Fitted equations for predicting the k_{600} (m d^{-1}) based on stream velocity (V , in m s^{-1}), slope (S ; unitless), depth (D , in meters), discharge (Q , in $\text{m}^3 \text{s}^{-1}$), and the Froude number ($Fr = V/(gD)^{0.5}$). Also displayed are the standard deviations (± 1 SD) for the equation parameters, r^2 , slope ($\pm \text{SE}$), and y -intercept ($\pm \text{SE}$ for regressions of the equation output vs. actual values; Fig. 3). All p -values for the regressions are 0.0001.

Model equation	r^2	Slope	y -Intercept
1. $k_{600} = (VS)^{0.89 \pm 0.0020} \times D^{0.54 \pm 0.030} \times 5037 \pm 604$	0.72	0.92 ± 0.024	0.98 ± 0.17
2. $k_{600} = 5937 \pm 606 \times (1 - 2.54 \pm 0.223 \times Fr^2) \times (VS)^{0.89 \pm 0.017} \times D^{0.58 \pm 0.027}$	0.76	0.94 ± 0.022	0.76 ± 0.16
3. $k_{600} = 1162 \pm 192 \times S^{0.77 \pm 0.028} V^{0.85 \pm 0.045}$	0.54	0.91 ± 0.036	0.91 ± 0.24
4. $k_{600} = (VS)^{0.76 \pm 0.027} \times 951.5 \pm 144$	0.53	0.82 ± 0.037	0.92 ± 0.24
5. $k_{600} = VS \times 2841 \pm 107 + 2.02 \pm 0.209$	0.55	1.0 ± 0.038	$-4.8 \times 10^{-3} \pm 0.26$
6. $k_{600} = 929 \pm 141 \times (VS)^{0.75 \pm 0.027} \times Q^{0.011 \pm 0.016}$	0.53	0.92 ± 0.036	0.81 ± 0.24
7. $k_{600} = 4725 \pm 445 \times (VS)^{0.86 \pm 0.016} \times Q^{-0.14 \pm 0.012} \times D^{0.66 \pm 0.029}$	0.76	0.95 ± 0.023	0.57 ± 0.17

- K_{600} is a function of turbulence at the surface of streams
- Calculated from slope and velocity (Raymond et al. 2012)
- Velocity estimated from discharge and hydraulic equations
- Slope gathered from Hydrosheds

$$V = cQ^d$$

NARWidth (Allen and Pavelsky 2015)



Global River Width from Landsat (GRWL) Database

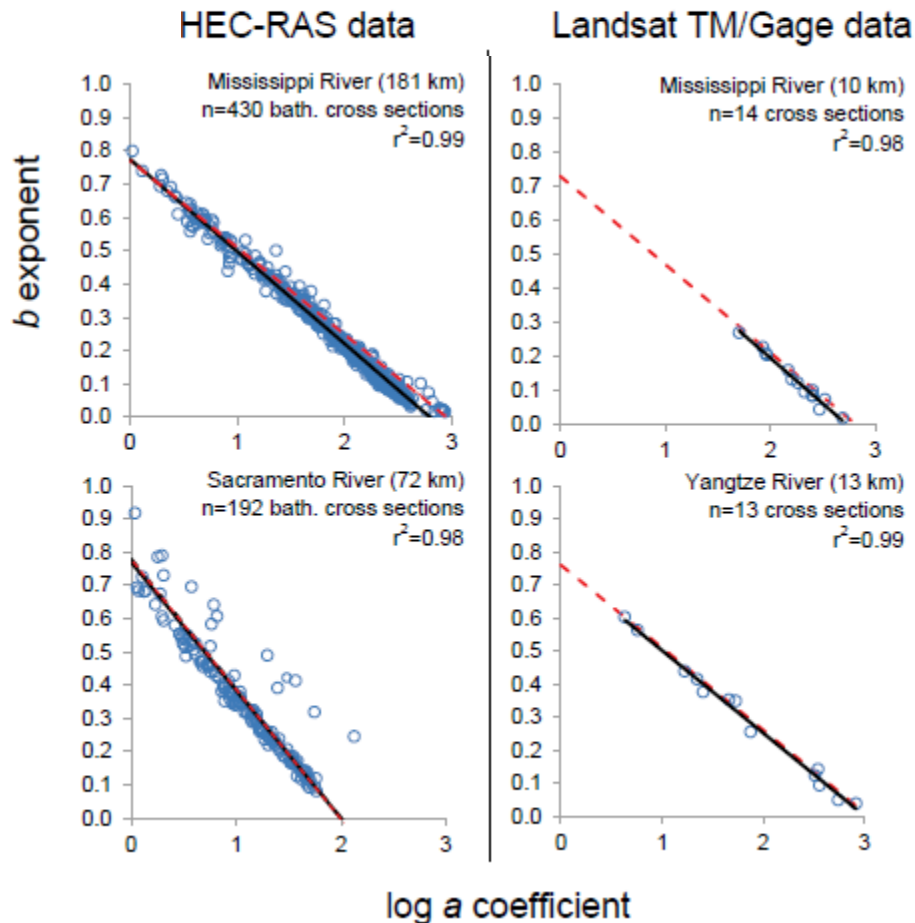


Toward global mapping of river discharge using satellite images and at-many-stations hydraulic geometry

Colin J. Gleason¹ and Laurence C. Smith

Department of Geography, University of California, Los Angeles, CA 90095-1524

Edited by James S. Famiglietti, University of California, Irvine, CA, and accepted by the Editorial Board February 18, 2014 (received for review September 17, 2013)



Significance

Political and practical realities limit our knowledge of water resources in many parts of the world. Here, we present a radically different approach for quantitative remote sensing of river discharge (flow rate) that is enabled by advancing a classic theory of river hydraulics and adapting it for use with satellite or aerial images. Because no ground-based information is required, the approach holds promise for addressing pressing societal, ecological, and scientific problems through global mapping of river flow.



RESEARCH LETTER

10.1002/2014GL060641

A global inventory of lakes based on high-resolution satellite imagery

Charles Verpoorter^{1,2}, Tiit Kutser^{2,3}, David A. Seekell^{4,5}, and Lars J. Tranvik²

¹INSU-CNRS, UMR 8187, LOG, Laboratoire d'Océanologie et des Géosciences, Université du Littoral Côte d'Opale, ULCO, Wimereux, France, ²Department of Ecology and Genetics/Limnology, Uppsala University, Uppsala, Sweden, ³Estonian Marine Institute, University of Tartu, Tallinn, Estonia, ⁴Department of Environmental Sciences, University of Virginia, Charlottesville, Virginia, USA, ⁵Now at Department of Ecology and Environmental Sciences, Umeå University, Umeå, Sweden

Key Points:

- Earth has 117 million lakes > 0.002 km²
- Large and intermediate lakes dominate the total surface area of lakes
- Power law-based extrapolations do not adequately estimate lake abundance

Remote sensing analysis

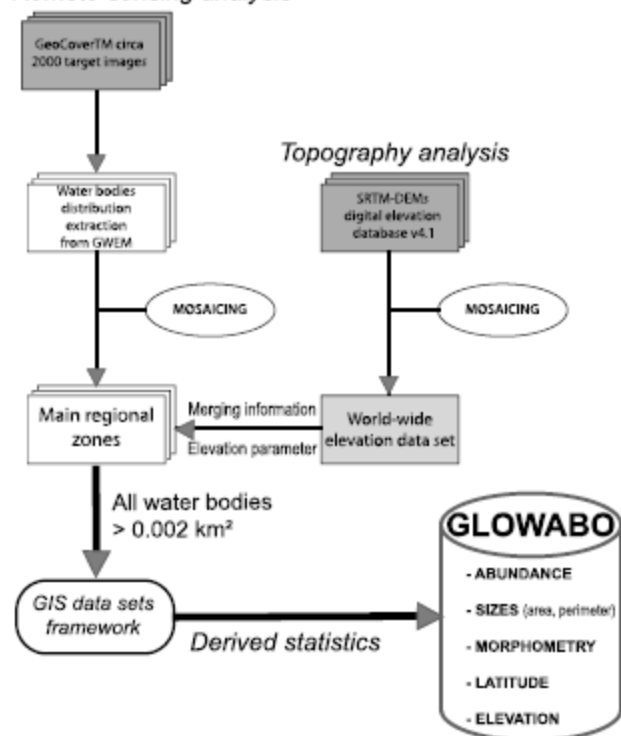
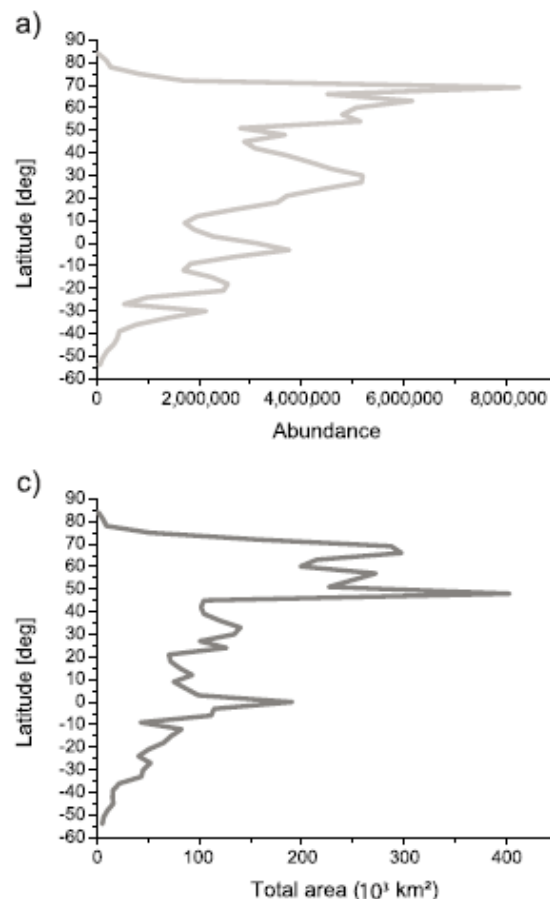


Figure 1. Overview of GLOWABO computations showing the data set inputs used (grey boxes), the data set outputs generated (white boxes), and the methodology used (GWEM).



Monitoring flood extent in the lower Amazon River floodplain using ALOS/PALSAR ScanSAR images

Allan S. Arnesen^{a,*}, Thiago S.F. Silva^a, Laura L. Hess^b, Evelyn M.L.M. Novo^a, Conrado M. Rudorff^c, Bruce D. Chapman^d, Kyle C. McDonald^{d,e}

^a Divisão de Sensoriamento Remoto, Instituto Nacional de Pesquisas Espaciais, Caixa Postal 515, 12201-970, São José dos Campos, Brazil

^b Earth Research Institute, 6832 Ellison Hall, University of California, Santa Barbara, CA 93106-3060, USA

^c Bren School of Environmental Science & Management, 2400 Bren Hall, University of California, Santa Barbara, CA 93106-5131 USA

^d Jet Propulsion Laboratory, California Institute of Technology, Pasadena, CA 91109, USA

^e Department of Earth and Atmospheric Sciences, CUNY Environmental Crossroads Initiative, and CUNY CREST Institute, City College of New York, City University of New York, 160 Convent Ave. & W. 138th St., New York, NY 10031, USA

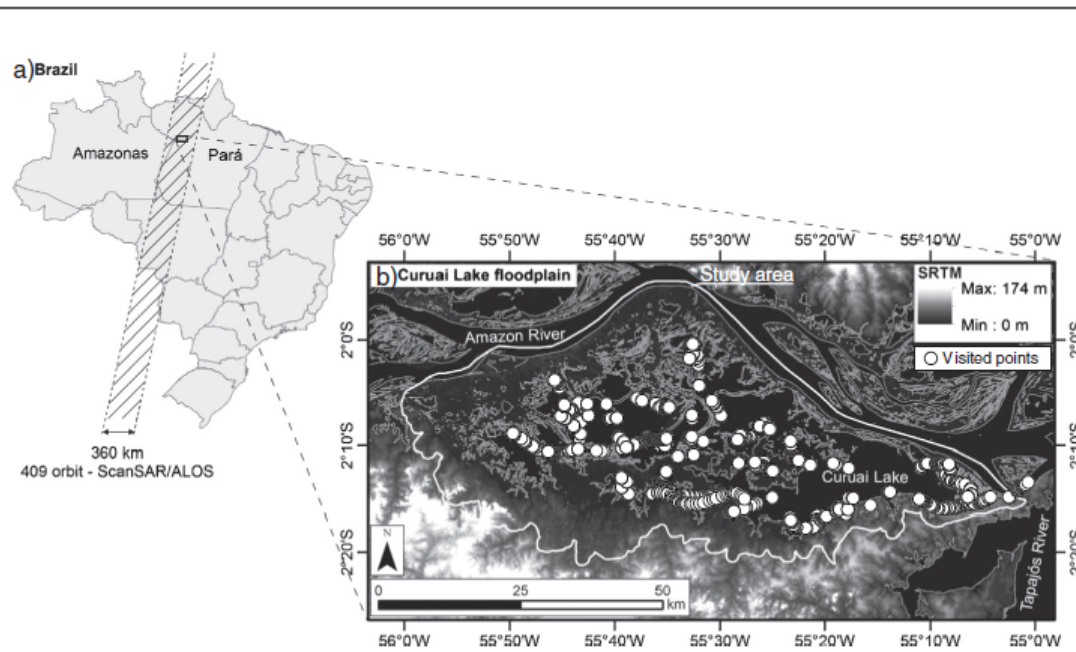


Fig. 1. Curuai Lake floodplain, Lower Amazon River, Pará state, Brazil. a) Hatched area represents the 409 ScanSAR/ALOS orbit; b) Curuai Lake floodplain; the white line indicates boundaries of the study area and white dots represent field locations visited during the rising water stage of 2011 (April). Background is SRTM digital elevation model.

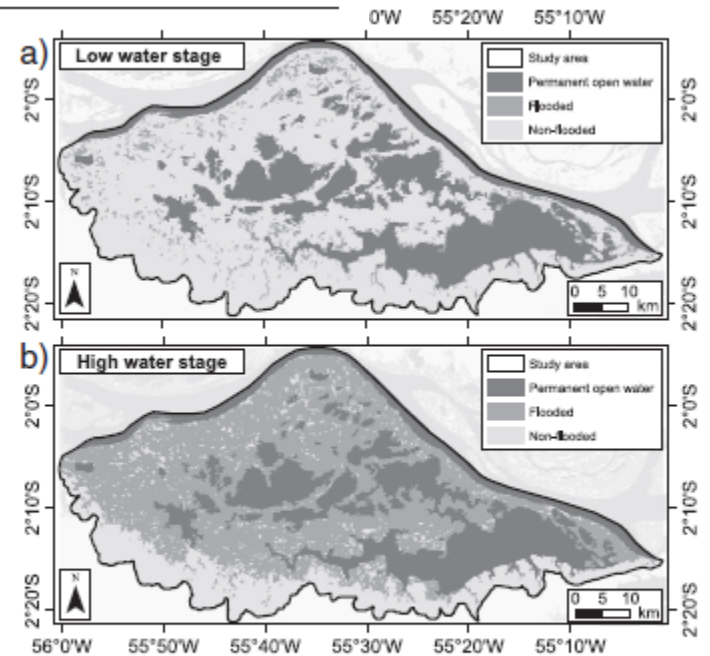


Fig. 8. Flood extent mapped for the Curuai Lake floodplain (Lower Amazon River, Brazil) for two dates: 2006-11-30 representing the low water stage (a) and 2007-07-18 representing the high water stage (b). The black line indicates the polygon considered for flooded area calculations.

Conclusions

- Inland waters transport terrestrial material to the ocean but are also sites of active processing
- Ability to efficiently and accurately measure land to water transfers improving greatly
- Models will be able to use this new data to link hydrology and terrestrial components
- Refined estimates of surface area of inland waters needed and are occurring.